HHS Public Access

Author manuscript

Eur Radiol. Author manuscript; available in PMC 2019 January 22.

Published in final edited form as:

Eur Radiol. 2013 February ; 23(2): 579–587. doi:10.1007/s00330-012-2631-y.

Prognostic implications of the magnetic resonance imaging appearance in papillary renal cell carcinoma

Andrew B. Rosenkrantz,
Department of Radiology, NYU Langone Medical Center,560 First Avenue TCH-HW202, New York, NY 10016, USA Andrew.Rosenkrantz@nyumc.org

Aarti Sekhar,
Department of Radiology, Beth Israel Deaconess Medical Center,330 Brookline Avenue,Boston, MA 02118, USA

Elizabeth M. Genega,
Department of Pathology, Beth Israel Deaconess Medical Center,330 Brookline Avenue,Boston, MA 02118, USA

Jonathan Melamed,
Department of Pathology, NYU Langone Medical Center, 550 First Avenue,New York, NY 10016, USA

James S. Babb,
Department of Radiology, NYU Langone Medical Center,560 First Avenue TCH-HW202, New York, NY 10016, USA

Amish D. Patel,
Department of Radiology, Beth Israel Deaconess Medical Center,330 Brookline Avenue,Boston, MA 02118, USA

Andy Lo,
Department of Pathology, NYU Langone Medical Center, 550 First Avenue,New York, NY 10016, USA

Robert M. Najarian,
Department of Pathology, Beth Israel Deaconess Medical Center,330 Brookline Avenue,Boston, MA 02118, USA

Muneeb Ahmed, and
Department of Radiology, Beth Israel Deaconess Medical Center,330 Brookline Avenue,Boston, MA 02118, USA

Ivan Pedrosa
Department of Radiology, Beth Israel Deaconess Medical Center,330 Brookline Avenue,Boston, MA 02118, USA

*Present Address:*A. Sekhar, Department of Radiology, Emory University Hospital, 1364 Clifton Road, NE, Atlanta, GA 30322, USA
*Present Address:*I. Pedrosa, Department of Radiology, UT Southwestern Medical Center, Advanced Imaging Research Center, 5323 Harry Hines Boulevard, Dallas, TX 75390-9061, USA

Abstract

Objective—To evaluate the prognostic implications of the MRI appearance and pathological features of papillary renal cell carcinoma (pRCC).

Methods—A total of 128 pRCC in 115 patients who underwent preoperative MRI were characterised in terms of pathological type (type 1 vs. type 2), MRI appearance (focal vs. infiltrative)and additional MRI features. Patients were classified on the basis of the presence or absence of metastatic disease.

Results—There were 65 focal type 1, 54 focal type 2 and 9 infiltrative pRCC. All infiltrative pRCC were of histopathological type 2. Renal vein thrombus was present in 89 % of infiltrative pRCC and no cases of focal pRCC. Metastatic disease was observed in 3.7 % of focal type 1, 7.5 % of focal type 2 and 75.0 % of infiltrative type 2 pRCC. Infiltrative MRI appearance was a significant predictor of metastatic disease, independent of pathological type, size and T stage ($P \leq 0.020$). Among focal pRCC on MRI, pathological type 2 was not a significant predictor of metastatic disease (P00.648). No combination of features achieved significantly greater accuracy for predicting metastatic disease than renal vein thrombus alone ($P > 0.5$).

Conclusion—Infiltrative MRI appearance and renal vein thrombus identify a subset of pathological type 2 pRCC at a significantly increased risk of metastatic disease.

Keywords

Papillary; Renal cell carcinoma; MRI. Metastatic disease; Renal vein thrombus

Introduction

Papillary renal cell carcinoma (pRCC) is the second most common subtype of renal cell carcinoma (RCC), constituting 10–20 % of all cases [1–3]. Although several large series have found the papillary subtype to be an independent predictor of a favourable prognosis for RCC [1, 2, 4], a small fraction of cases exhibit a highly aggressive clinical course with a prognosis that is among the poorest of any subgroup of RCC [5–7]. In 1997, Delahunt and Eble proposed a pathological classification scheme that divides pRCC into two groups: type 1 tumours with cells with scant pale cytoplasm arranged as a single layer along a papillary core, and type 2 tumours with pseudostratified nuclei and voluminous eosinophilic cytoplasm [8]. Some studies have shown worse outcome for type 2 than for type 1 pRCC [5, 7, 9, 10], such that it is this group that is generally deemed to represent the more aggressive subtype of pRCC.

Despite the potential prognostic value of the Delahunt morphological classification system, its use remains controversial given the lack of supporting molecular evidence. In particular, overlap in the molecular and genetic features of type 1 and type 2 pRCC have been demonstrated [7, 11], and some cases of pRCC show morphological features of both type 1 and type 2 tumours [11]. Furthermore, not all studies have found the pathological classification to be a significant independent predictor of clinical outcome [12, 13]. Therefore, this classification system has not been universally applied across studies of pRCC [4, 14].

Magnetic resonance imaging (MRI) offers excellent soft tissue contrast and has shown high performance for the detection, characterisation and staging of renal masses [15–18]. More recently, MRI features have shown potential in the non-invasive identification of the histological subtype of RCC [19, 20]. In particular, two distinct MRI appearances of pRCC are characteristic and well-described [21]: a small peripheral T2-hypointense hypoenhancing solid mass, and a cystic lesion with haemorrhagic fluid and peripheral papillary projections, the latter probably resulting from intratumoural haemorrhage in solid masses. Rarely, pRCC may present on cross-sectional imaging with a third appearance: as a central, poorly circumscribed, infiltrative mass [22]. In our experience, it is this manifestation of pRCC that has a strong association with aggressive clinical behaviour. However, to our knowledge, no previous study has correlated the different MRI appearances of pRCC with their clinical outcome. Therefore, the purpose of this study was to compare the prognostic implications of the MRI appearance and pathological features in pRCC.

Materials and methods

Patients

This was a retrospective study involving two academic medical centres. Institutional review board approval was obtained at both centres, with waiver of requirement of written informed consent. The study was Health Insurance Portability and Accountability Act (HIPAA)-compliant. Institutional databases were searched to identify all cases of pathologically confirmed pRCC between January 2003 and December 2009 in which the patient underwent preoperative renal MRI. A total of 142 masses in 124 patients were identified. Fourteen masses were excluded at pathological analysis owing to missing slides (n=5), insufficient tissue (n=1), or reclassification as mixed papillary and clear-cell subtype (n=6), alternate RCC subtype other than papillary (n=1), or benign histology (i.e. oncocytoma) (n=1). This left a final cohort of 128 masses in 115 patients for inclusion in our study. All patients were imaged using a 1.5-T or 3-T clinical MRI system and a standard renal mass protocol that included axial and/orcoronal two-dimensional (2D) T2-weighted single-shot fast-spin echo, axial 2D in- and opposed-phase T1-weighted spoiled gradient echo; and 3D fat-suppressed T1-weighted spoiled gradient-echo sequences; the latter sequence was performed before and during corticomedullary, nephrographic and excretory phases following the administration of gadolinium chelate in the axial, coronal and/or sagittal planes. The specific acquisition parameters for these sequences at the two centres have been previously published [21, 23].

Histological analysis

All pathological specimens were reviewed by a single uropathologist at each institution (centre 1: EG, with 11 years' experience; centre 2: JM, with 22 years' experience), who was unaware of the MR findings and clinical outcomes. The pathologist confirmedthe diagnosis of pRCC foreach case and classified the tumour in terms of (1) Delahunt category [8]: pathological type 1 versus type 2; (2) most common nuclear grade: low (Fuhrman I–II) versus high (Fuhrman III–IV) grade; and (3) highest nuclear grade [24]: low (Fuhrman I–II) versus high (Fuhrman III–IV) grade. The T and N status, as determined by pathological assessment, was also recorded.

Image analysis

All imaging was reviewed by a single radiologist at each institution (centre 1: IP, with 10 years of experience in body MR imaging; centre 2: AR, with 2 years' experience in body MR imaging), who was unaware of pathological findings and clinical outcomes. All masses were classified in terms of previously described MRI features [20]: location (central vs. peripheral); T2 signal intensity (SI) (hyper-, iso- or hypointense relative to renal cortex); uniformity of T2 SI (homogeneous or heterogeneous); cystic component (present or absent); intracellular lipids (present or absent); haemosiderin (present or absent); haemorrhage (present or absent); necrosis (present or absent); enhancement uniformity (homogeneous or heterogeneous); enhancement on nephrographic phase (hyper-, iso- or hypovascular relative to renal cortex); encapsulation (well or poorly encapsulated); margins (entirely smooth margins or at least focal irregularity); retroperitoneal collaterals (present or absent); perirenal fat invasion (present or absent); and renal vein thrombosis (present or absent). MRI features were classified on the basis of the predominant component of the mass. The maximal diameter of each lesion was also recorded. Each mass was also classified in terms of one of three appearances on MRI: (I) focal encapsulated solid hypoenhancing mass; (II) focal encapsulated cystic lesion containing T1-hyperintense (i.e. haemorrhagic) fluid and peripheral papillary projections; (III) infiltrative poorly circumscribed central mass (Figs. 1, 2 and 3).

Clinical outcomes

Each patient was classified in terms of either the presence or absence of metastatic disease on the basis of review of follow-up contrast-enhanced cross-sectional imaging (CT or MRI) of the abdomen and review of oncologist clinic notes. In cases in which the retrospective chart review indicated metastatic disease, the location of metastases and duration from diagnosis to metastatic disease were recorded. At least 1-year follow-up was required to classify a patient in terms of the absence of metastatic disease. Patients without definitive evidence of meta-static disease but with less than 1-year follow-up were considered indeterminate regarding the presence of metastatic disease. The development of pulmonary embolism was considered to represent metastatic disease in patients with renal vein tumour thrombus. The development of metachronous solid renal masses following resection of the initial pRCC was recorded but not considered to represent metastatic disease.

Statistical analysis

Tumours were divided into three pRCC categories: focal type 1 (MRI appearance I or II and pathological type 1), focal type 2 (MRI appearance I or II and pathological type 2) or infiltrative (MRI appearance III, either pathologicaltype). Mixed model analysis of variance (ANOVA) was used to compare types of pRCC and sites of accrual in terms of size. Lesion size was the dependent variable and the model included site and type as fixed classification factors. Generalised estimating equations (GEE) based on a binarylogistic regression model were used to test the association of tumour type with accrual site and each imaging feature. The indicator of type was the dependent variable and each model included site and exactly one imaging feature as classification factors. GEE were also used to compare sites with respect to each categorical factor and to assess whether renal vein throm-bus was more

prevalent for infiltrative pRCC than other lesions. For both ANOVA and GEE, the correlation structure was modelled by assuming results to be correlated only when acquired from the same patient. For ANOVA, the error variance was allowed to differ across lesion types to remove the assumption of variance homogeneity. The above analyses included data from all patients.

Analysis to identify predictors of metastatic disease only used data from patients for whom there was a reference standard assessment of metastases. As the presence/absence of metastatic disease is a subject-level factor, lesion size was recorded for each patient as the maximum over lesions and each categorical factor was represented by an indicator of at least one lesion with the characteristic that was optimal for predicting metastatic disease. Univariate and multivariate binary logistic regression analyses were used to identify individual factors predictive of metastases and to identity subsets of independent predictors of metastases, respectively. McN-emar's tests were used to compare MRI appearance III with pathological type 2 in terms of accuracy for detection of metastases. Kaplan–Meier survival curves and log-rank test were used to characterise and compare different subsets of pRCC in terms of progression-free survival (PFS). The Wald test for type 3 GEE analysis was used to assess whether MRI appearance significantly improved the accuracy for the prediction of metastatic disease compared with pathological type, T status and lesion size, respectively. For all GEE analyses involving Tstage, categories T2 and T3 were combined given the small number of lesions classified as T2. All analyses are two-sided and considered statistically significant at $P<0.05$.

Results

Patients and lesions

Table 1 shows baseline features for 128 renal masses in 115 patients. At histopathology, 65 masses were classified as type 1 and 63 as type 2. Eighty-three, 36 and 9 masses were classified as exhibiting MRI appearances I, II and III, respectively. All 9 masses characterised as MRI appearance III (i.e. infiltrative) were classified as pathological type 2. When combining the pathological and MRI designations, 65 masses were classified as focal type 1 pRCC, 54 as focal type 2 pRCC and 9 as infiltrative pRCC. Table 2 provides a comparison of the imaging and pathological features of these three categoriesof pRCC. There was no significant difference between tumours from centre 1 and centre 2 in terms of T stage ($P=0.325$), tumour size ($P=0.512$), MRI category ($P=0.902$), pathological type ($P=0.373$),or any of the other categorical imaging or pathological variables ($P>0.5$).

Association with metastatic disease

Metastatic disease was categorised as present in 11 patents, absent in 78 and indeterminate in 26. In patients without metastatic disease, the mean follow-up was 3.9±1.9 years (range 1.0–8.0 years, median 3.6 years). In patients with metastatic disease, the mean time from diagnosis to metastatic disease was 0.9±1.6 years (range 0–4.6 years, median 0.1 years). Five of the 11 patients with metastatic disease had metastatic disease at the time of initial diagnosis. Metastases were identified within the following locations: liver ($n=3$), lung ($n=3$), lymph nodes ($n=5$), bone ($n=1$) and pulmonary embolus in the presence of renal vein tumour

thrombus (n=3). Four patients developed a separate solid enhancing renal mass after the initial diagnosis of pRCC, which was not categorised as metastatic disease.

Features associated with metastatic disease at univariate analysis include higher stage, larger size, central location, poor encapsulation, irregular margin, perirenal invasion, retroperitoneal collaterals, renal vein thrombus, predominantly high nuclear grade, pathological type 2 and infiltrative MRI appearance (P values ranging from less than 0.001 to 0.027). All other factors were not significant predictors of metastatic disease (P values ranging from 0.085 to 1.0). Lesions associated with metastatic disease ranged in size from 43 to 110 mm. Overall highest accuracy for the detection of metastatic disease in terms of lesion size was achieved using a threshold of 68 mm (accuracy of 91.1 %). Table 3 shows the accuracy, sensitivity, specificity and odds ratio associated with each factor identified as a significant predictor of metastatic disease at univariate analysis.

Metastatic disease was observed in 3.7 % of focal type 1, 7.5 % of focal type 2 and 75.0 % of infiltrative type 2 pRCC. The frequency of metastatic disease in infiltrative pRCC was significantly greater than that in focal type 1 and focal type 2 pRCC combined (P<0.001), although not significantly different between focal type 1 and focal type 2 pRCC (P=0.648). Use of infiltrative appearance on MRI as a predictor of metastatic disease, in comparison with pathological type 2, demonstrated greater accuracy (P<0.001) and specificity (P<0.001), with no significant difference in terms of sensitivity (P=0.250). In addition, when both infiltrative appearance on MRI and pathological type 2 were included in a single model to predict metastases, the partial P values, each adjusted for the other measure, for infiltrative appearance and for pathological type 2 were 0.001 and 0.4963, respectively; when both infiltrative appearance on MRI and stage T2/T3 were included in a single model, the partial P values for infiltrative appearance and for stage T2/ T3 were 0.020 and 0.059, respectively; and when both infiltrative appearance on MRI and lesion size were included in a single model, the partial P values for infiltrative appearance and for lesion size were 0.014 and 0.105,respectively. These results indicate that the inclusion of MRI appearance significantly increased the accuracy of the prediction of metastatic disease compared with pathological type, T stage or size alone, respectively.

Figure 4 shows PFS curves among different subsets of pRCC. Median PFS for infiltrative MRI appearance was 0.534 years, which was significantly worse than that for other categories of pRCC combined (P<0.001). While PFS was significantly worse among patients with pathological type 2 than pathological type 1 pRCC (0.043), there was no significant difference in PFS between focal type 1 pRCC and focal type 2 pRCC (0.633) or between MRI appearances I and II (P00.179). There were too few patients manifesting metastatic disease during follow-up to estimate median PFS among subgroups other than infiltrative pRCC.

Renal vein thrombus was present in 89 % of cases of infiltrative pRCC (8/9) but in 0/65 cases of focal type 1 pRCC and in 0/54 cases of focal type 2 pRCC. Renal vein invasion was significantly more prevalent among infiltrative type pRCC than among all other pRCC (P<0.0001). All three patients with pulmonary embolism had infiltrative pRCC. At univariate analysis, renal vein thrombus had the highest odds ratio (108.0) of any measure in

the prediction of metastatic disease. Multivariate logistic regression analyses identified no set of two or more measures that were significant independent predictors of metastases that together achieved greater overall diagnostic accuracy than renal vein thrombus alone (P>0.5).

Discussion

Although pRCC is generally considered to have a favourable prognosis, this tumour can exhibit a highly aggressive clinical course in a subset of cases [2, 5]. While both the Fuhrman nuclear grading system and the system described by Delahunt (type 1 vs. type 2) have been applied for the prediction of outcome of pRCC, the performance of these systems has been variable across studies [10, 12, 25, 26]. In our study, there were clear prognostic implications of the MRI appearance of pRCC, independent of pathological features, size and stage. Most of the pRCC had a well-encapsulated appearance, which we have designated as focal pRCC, matching the typical imaging appearance of pRCC in previous reports [20]. However, a small fraction of pathological type 2 pRCC exhibited an infiltrative morphology on MRI, an appearance that we identified to have a substantially worse prognosis among cases of type 2 pRCC. In addition focal type 1 pRCC and focal type 2 pRCC exhibited a nearly indistinguishable appearance on MRI and a similar frequency of metastatic disease, countering the notion that the designation of type 2 pRCC, by itself, carries a worse prognosis.

While only observed in approximately 7 % of pRCC in this study, the presence of an infiltrative morphology on MRI was associated with poor prognosis, having a specificity of approximately 98 % for metastatic disease. The over-all accuracy for the identification of metastatic disease based on infiltrative morphology was 92 %, in comparison with an accuracy of 59 % based on the presence of pathological type 2 designation alone, and attempts to include both factors in a single model to predict metastases identified a stronger partial P value for the presence of infiltrative MRI appearance. Further supporting the clinical utility of infiltrative morphology as a prognostic marker is the ease with which this appearance can be recognised. Conversely, a known limitation of the pathological classification system is over-lapping features of type 1 and type 2 pRCC [11].

Furthermore, in our series, neither lesion size nor T stage was a significant independent predictor of metastatic disease when combined in a multivariate model with MRI appearance of pRCC.

A particularly strong association of infiltrative pRCC with venous thrombus was noted in our study. Renal vein invasion was present in 89 % of infiltrative pRCC in comparison with no cases of focal pRCC. In addition, three patients with infiltrative pRCC and renal vein thrombus developed pulmonary embolus, which has previously been postulated to be the mechanism of virulence for those cases of pRCC with an aggressive clinical course: Margulis et al. observed venous tumour thrombus to be associated with drastically decreased survival for pRCC but not for clear-cell RCC (ccRCC); in their study, venous thrombus had a risk ratio for the prediction of disease-specific mortality of 17.8 and 2.8 for pRCC and ccRCC, respectively [6]. While Yamada et al. also identified a central infiltrative

morphology with a propensity for venous thrombus in cases of type 2 pRCC in a study using CT [11], these authors did not compare the imaging features among cases of pRCC with clinical outcomes.

Although requiring prospective validation, the association that we observed between the infiltrative MRI appearance of a small subset of type 2 pRCC and metastatic disease would facilitate the role of MRI as a non-invasive prognostic marker for pRCC. For instance, patients with type 2 pRCC exhibiting infiltrative MRI appearance, particularly when presenting with renal vein thrombus, may represent candidates for adjuvant chemotherapy should an effective treatment for stage IV disease become available, given the much greater risk of metastatic disease in these cases.

Several limitations of our study warrant mention. First, this was a retrospective study with only a small number of patients who developed metastatic disease. Second, our criteria for the absence of metastatic disease may be considered short at only 1 year. Third, although strong differences were seen in terms of metastatic disease between the different MRI appearances, they did not correlate with patient survival. Fourth, we have not correlated the different MRI patterns that we describe with differences in molecular or genetic features.

Finally, details of the acquisition parameters of the MRI examination varied slightly between the two institutions. How-ever, we doubt that this hadan impact on ourFindings given the absence of a significant difference in the distribution of any of the assessed imaging features between the two centres.

In conclusion, we have identified an association between the MRI appearance of pRCC and metastatic disease. Specifically, among cases of pathological type 2 pRCC, those with infiltrative MRI appearance were at a substantially increased risk of metastatic disease, independent of tumour stage, size and grade. There was also a high frequency of venous thrombus among cases of infiltrative type 2 pRCC. Focal type 1 pRCC and focal type 2 pRCC had similar imaging features on MRI and no difference in frequency of metastatic disease. Although requiring prospective validation, our findings suggest the potential role of MRI appearance in prognosis, patient counselling and treatment planning for pRCC.

Acknowledgments

We would like to acknowledge Dr. Michael B. Atkins for assistance in reviewing this manuscript.

References

1. Amin MB, Tamboli P, Javidan J et al. (2002) Prognostic impact of histologic subtyping of adult renal epithelial neoplasms: an experience of 405 cases. Am J Surg Pathol 26:281–291 [PubMed: 11859199]
2. Cheville JC, Lohse CM, Zincke H, Weaver AL, Blute ML (2003) Comparisons of outcome and prognostic features among histologic subtypes of renal cell carcinoma. Am J Surg Pathol 27:612–624 [PubMed: 12717246]
3. Leroy X, Zini L, Leteurtre E et al. (2002) Morphologic subtyping of papillary renal cell carcinoma: correlation with prognosis and differential expression of MUC1 between the two subtypes. Mod Pathol 15:1126–1130. doi:10.1097/01.MP.0000036346.88874.25 [PubMed: 12429790]

4. Teloken PE, Thompson RH, Tickoo SK et al. (2009) Prognostic impact of histological subtype on surgically treated localized renal cell carcinoma. J Urol 182:2132–2136 [PubMed: 19758615]
5. Pignot G, Elie C, Conquy S et al. (2007) Survival analysis of 130 patients with papillary renal cell carcinoma: prognostic utility of type 1 and type 2 subclassification. Urology 69:230–235 [PubMed: 17275070]
6. Margulis V, Tamboli P, Matin SF, Swanson DA, Wood CG (2008) Analysis of clinicopathologic predictors of oncologic outcome provides insight into the natural history of surgically managed papillary renal cell carcinoma. Cancer 112:1480–1488 [PubMed: 18240184]
7. Allory Y, Ouazana D, Boucher E, Thiounn N, Vieillefond A (2003) Papillary renal cell carcinoma. Prognostic value of morphological subtypes in a clinicopathologic study of 43 cases. Virchows Arch 442:336–342 [PubMed: 12684768]
8. Delahunt B, Eble JN (1997) Papillary renal cell carcinoma: a clinicopathologic and immunohistochemical study of 105 tumors. Mod Pathol 10:537–544 [PubMed: 9195569]
9. Delahunt B, Eble JN, McCredie MR, Bethwaite PB, Stewart JH,Bilous AM (2001) Morphologic typing of papillary renal cell carcinoma: comparison of growth kinetics and patient survival in 66 cases. Hum Pathol 32:590–595 [PubMed: 11431713]
10. Yamashita S, Ioritani N, Oikawa K, Aizawa M, Endoh M, Arai Y(2007) Morphological subtyping of papillary renal cell carcinoma: clinicopathological characteristics and prognosis. Int J Urol 14:679–683 [PubMed: 17681054]
11. Yang XJ, Tan MH, Kim HL et al. (2005) A molecular classification of papillary renal cell carcinoma. Cancer Res 65:5628–5637 [PubMed: 15994935]
12. Ku JH, Moon KC, Kwak C, Kim HH, Lee SE (2009) Is there a role of the histologic subtypes of papillary renal cell carcinoma as a prognostic factor? Jpn J Clin Oncol 39:664–670 [PubMed: 19586962]
13. Gontero P, Ceratti G, Guglielmetti S et al. (2008) Prognostic factors in a prospective series of papillary renal cell carcinoma. BJU Int 102:697–702 [PubMed: 18489525]
14. Schrader AJ, Rauer-Bruening S, Olbert PJ et al. (2009) Incidence and long-term prognosis of papillary renal cell carcinoma. J Cancer Res Clin Oncol 135:799–805 [PubMed: 19023595]
15. Semelka RC, Hricak H, Stevens SK, Finegold R, Tomei E, CarrollPR (1991) Combined gadolinium-enhanced and fat-saturation MR imaging of renal masses. Radiology 178:803–809 [PubMed: 1994422]
16. Pretorius ES, Siegelman ES, Ramchandani P, Cangiano T, BannerMP (1999) Renal neoplasms amenable to partial nephrectomy: MR imaging. Radiology 212:28–34 [PubMed: 10405716]
17. Ergen FB, Hussain HK, Caoili EM et al. (2004) MRI for preoperative staging of renal cell carcinoma using the 1997 TNM classification: comparison with surgical and pathologic staging. AJR Am J Roentgenol 182:217–225 [PubMed: 14684543]
18. Israel GM, Hindman N, Bosniak MA (2004) Evaluation of cystic renal masses: comparison of CT and MR imaging by using the Bosniak classification system. Radiology 231:365–371 [PubMed: 15128983]
19. Sun MR, Ngo L, Genega EM et al. (2009) Renal cell carcinoma: dynamic contrast-enhanced MR imaging for differentiation of tumor subtypes–correlation with pathologic findings. Radiology 250:793–802 [PubMed: 19244046]
20. Pedrosa I, Chou MT, Ngo L et al. (2008) MR classification of renal masses with pathologic correlation. Eur Radiol 18:365–375 [PubMed: 17899106]
21. Pedrosa I, Sun MR, Spencer M et al. (2008) MR imaging of renal masses: correlation with findings at surgery and pathologic analysis. Radiographics 28:985–1003 [PubMed: 18635625]
22. Yamada T, Endo M, Tsuboi M et al. (2008) Differentiation of pathologic subtypes of papillary renal cell carcinoma on CT. AJR Am J Roentgenol 191:1559–1563 [PubMed: 18941101]
23. Rosenkrantz AB, Hindman N, Fitzgerald EF, Niver BE, Melamed J,Babb JS (2010) MRI features of renal oncocytoma and chromophobe renal cell carcinoma. AJR Am J Roentgenol 195:W421–W427 [PubMed: 21098174]
24. Lang H, Lindner V, de Fromont M et al. (2005) Multicenter determination of optimal interobserver agreement using the Fuhrman grading system for renal cell carcinoma: assessment of 241 patients with >15-year follow-up. Cancer 103:625–629 [PubMed: 15611969]

25. Klatte T, Anterasian C, Said JW et al. (2010) Fuhrman grade provides higher prognostic accuracy than nucleolar grade for papillary renal cell carcinoma. J Urol 183:2143–2147 [PubMed: 20399450]

26. Sika-Paotonu D, Bethwaite PB, McCredie MR, William Jordan T,Delahunt B (2006) Nucleolar grade but not Fuhrman grade is applicable to papillary renal cell carcinoma. Am J Surg Pathol 30:1091–1096 [PubMed: 16931953]

Key Points

- Magnetic resonance imaging (MRI) offers new preoperative insights into renal cell carcinoma (RCC).
- Certain MRI features are associated with metastatic papillary RCC.
- Metastases seem more common given an infiltrative appearance and renal vein thrombus.

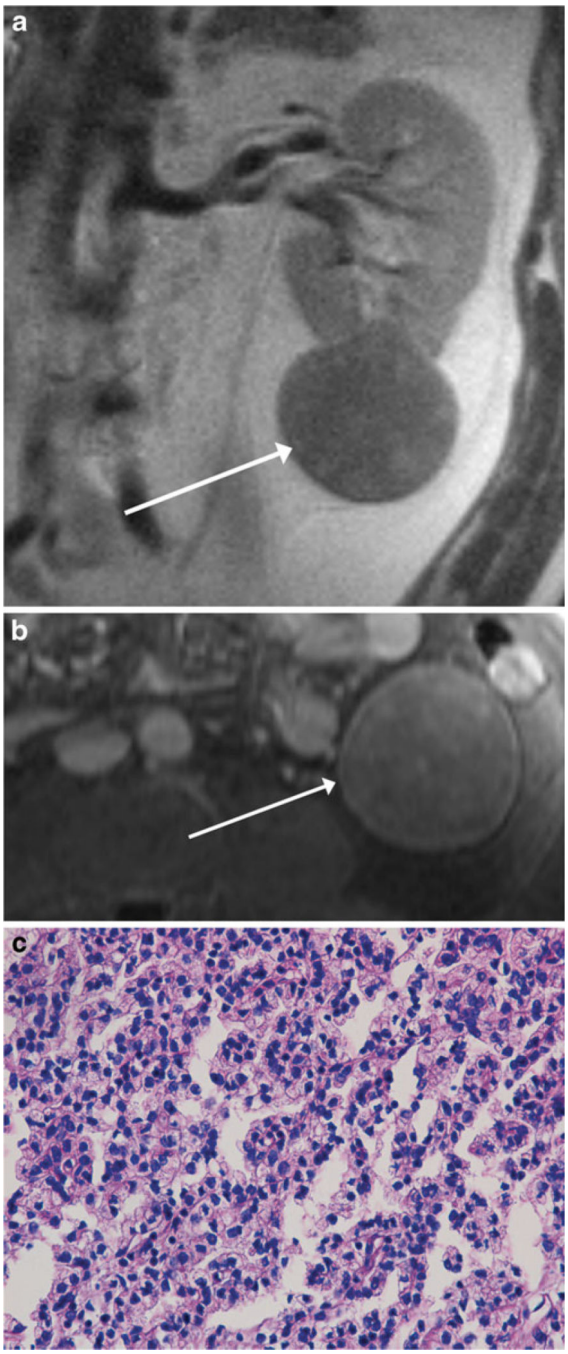

Fig. 1.

MR images of a 51-year-old man with a renal mass. Coronal single-shot T2-weighted image (a) and axial post-contrast fat-suppressed T1-weighted image (b) show a well-encapsulated T2-hypointense solid mass extending exophytically from the left lower pole (*arrow*). The mass showed diffuse low-level internal enhancement on subtracted post-contrast images (not shown). The findings were consistent with MRI appearance I. Mass was diagnosed as type 1 papillary renal cell carcinoma (pRCC) at partial nephrectomy and was therefore classified as focal type 1 pRCC in our study. Section of tumour (c) shows a relatively solid area of

tumour with small neoplastic nuclei without prominent nucleoli, indicative of low nuclear grade (H&E stain, ×400); overall, the lesion was classified as being of predominantly low nuclear grade, with high nuclear grade present (not shown). On follow-up cross-sectional imaging 7.0 years later, there was no evidence of metastatic disease

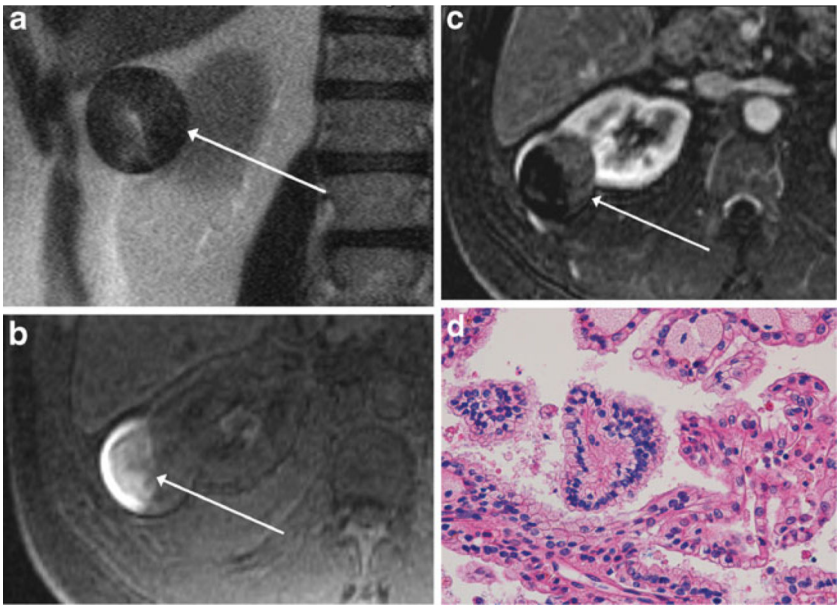

Fig. 2.

MR images of a 55-year-old man with a renal mass. Axial single-shot T2-weighted image (a), axial pre-contrast fat-suppressed T1-weighted image (b) and subtracted axial post-contrast fat-suppressed T1-weighted image (c) show a heterogeneous, predominantly T2 hypointense mass, extending exophytically from the lateral right kidney (*arrow*, a). There is T1 hyperintensity within the lateral aspect of the mass (*arrow*, b), indicative of haemorrhagic content, as well as low-level enhancement within the medial non-haemorrhagic portion of the mass (*arrow*, c), findings consistent with MRI appearance II. Mass was diagnosed as type 2 papillary renal cell carcinoma (pRCC) at partial nephrectomy and was therefore classified as focal type 2 pRCC in our study. Section of the tumour (d) shows papillary fronds lined by neoplastic cells with small nuclei (*centre* of the field), indicative of low nuclear grade, compared with a minor component on the *right-hand side* of the image with larger nuclei and conspicuous nucleoli, indicative of focal high nuclear grade (H&E stain, x400); overall, the lesion was classified as predominantly low nuclear grade, with high nucleargrade present. On follow-up cross-sectional imaging 4.9 years later, there was no evidence of metastatic disease

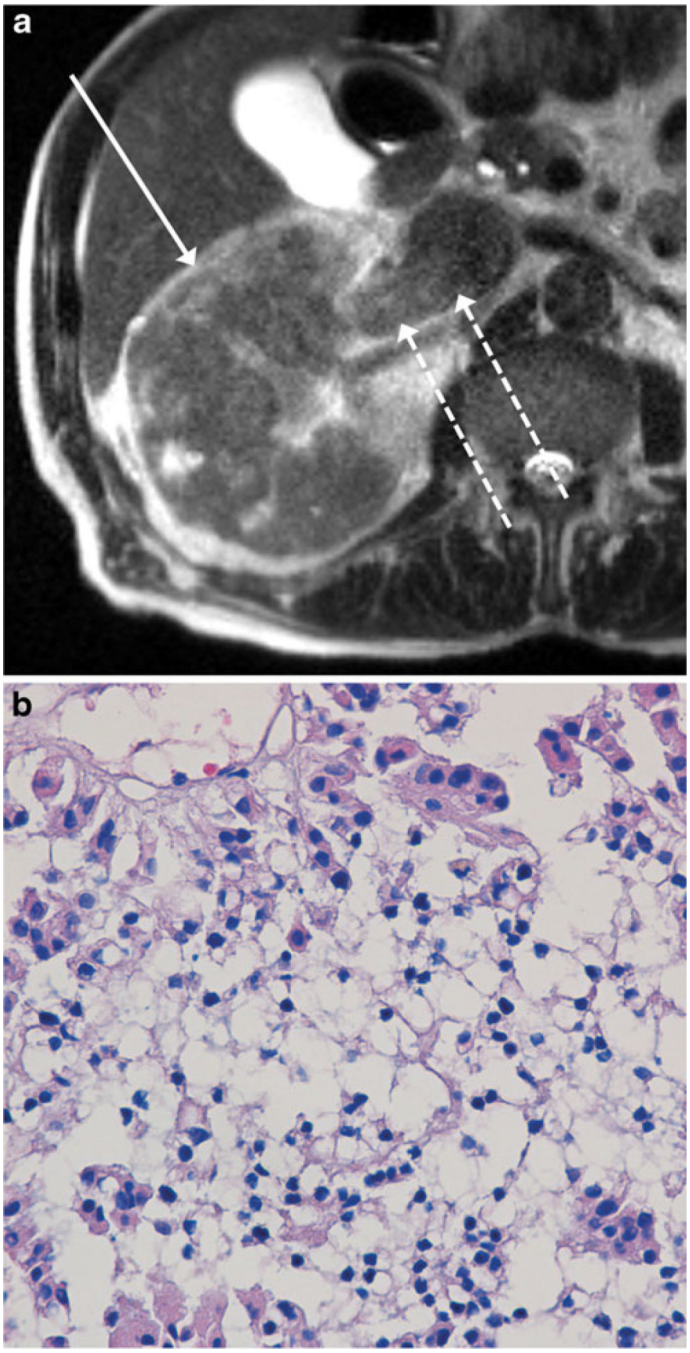

Fig. 3.

MR images of a 79-year-old man with a renal mass. Axial single-shot T2-weighted image (**a**) shows a large T2-hypointense poorly encapsulated infiltrative mass involving nearly the entire right renal parenchyma (*solid arrow*), consistent with MRI appearance III. There is also tumour thrombus throughout the right renal vein and extending into the inferior vena cava (IVC) (*dashed arrow*s). Although the mass was diagnosed as a type 2 papillary renal cell carcinoma (pRCC) at total nephrectomy, the mass was classified as infiltrative pRCC in our study. Section of tumour (**b**) shows a central area with small neoplastic nuclei without

prominent nucleoli, indicative of low nuclear grade, in comparison with focal areas at the periphery with larger nuclei and associated eosinophilic cytoplasm, indicative of high nuclear grade (H&E stain, x400); overall, the lesion was classified as predominantly low nuclear grade, with high nuclear grade areas present. Chest CT performed at the time of initial presentation (not shown) demonstrated a massive pulmonary embolus. In addition, nodal micrometastases were identified at the time of nephrectomy, although these were not evident on preoperative imaging

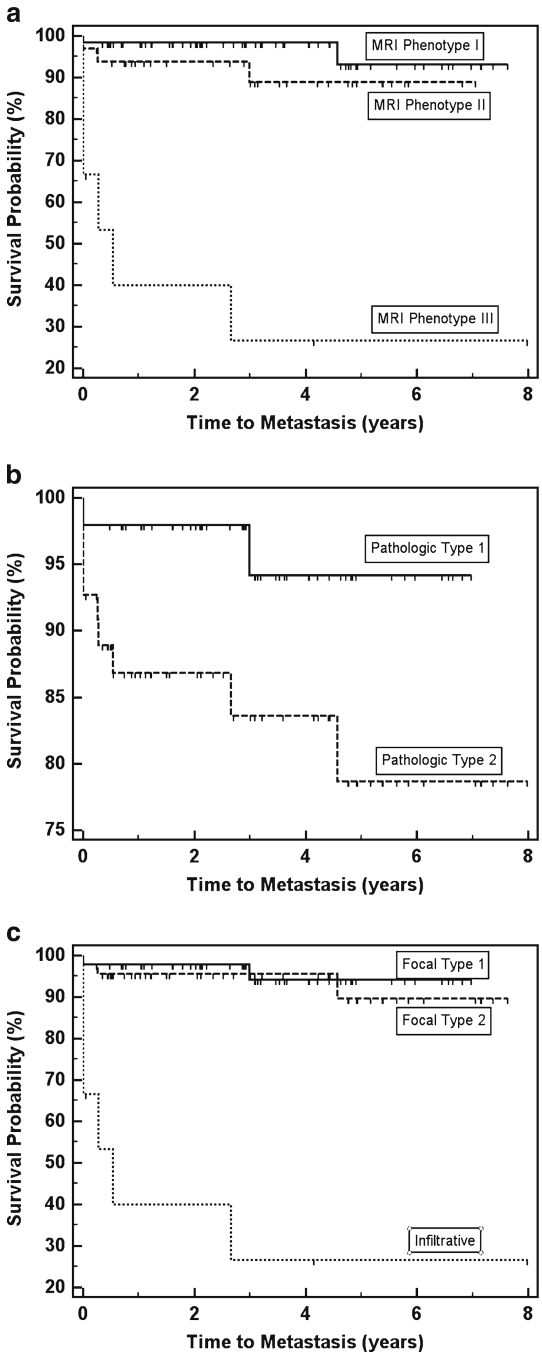

Fig. 4.

Kaplan–Meier progression-free survival (PFS) curves among patients with each MRI appearance (**a**), each pathological type (**b**) and overall type (**c**). Censored survival times are indicated by hash marks. MRI appearance III and overall type ‘infiltrative’ included the same patients and their estimated PFS was 0.534 years. A log-rank test showed significantly worse PFS among patients with pathological type 2 compared with pathological type 1 (*P*=0.043). There was no significant difference in PFS between MRI appearances I and II (*P*=0.179) or between focal types 1 and 2 (*P*=0.633). However, PFS was significantly worse

(P<0.001) for MRI appearance III (equivalent to overall ‘infiltrative’ type) than for the other categories combined

Table 1

Baseline characteristics of 128 lesions in 115 subjects

Gender[a]	94 men, 21	women
Age[a]		
Mean ± SD	62.2±11.6	
Median (range)	62	(28–90)
Site of accrual[a]		
Site 1	56	(49)
Site 2	59	(51)
Size[b]		
Mean ± SD	38.7±29.2	
Median (range)	28	(7–168)
Method of diagnosis[b]		
Total nephrectomy	79	(62)
Partial nephrectomy	42	(33)
Core biopsy of primary mass	5	(4)
Core biopsy of metastasis	2	(2)
T status[b]		
T1	93	(73)
T2	8	(6)
T3	20	(16)
T status unknown (mass not resected)	7	(5)
N status[a]		
N0	10	(9)
N1	2	(2)
N2	3	(3)
Nodes not histologically assessed	100	(87)
Pathological type[b]		
1	65	(51)
2	63	(49)
MRI appearance[b]		
I	83	(65)
II	36	(28)
III	9	(7)
Overall category[b]		
Focal type 1 pRCC	65	(51)
Focal type 2 pRCC	54	(42)
Infiltrative pRCC	9	(7)

Data m parentheses are percentages unless indicated otherwise

[a] Reported on a per-patient basis

[b] Reported on a per-lesion basis

Table 2

Frequency with which binary features were present in focal type 1, focal type 2 and infiltrative papillary renal cell carcinoma (pRCC), with *P* value obtained from univariate generalised estimating equations analysis for comparison between categories of pRCC

Feature	Focal type 1 pRCC[a]	Focal type 2 pRCC[a]	*P* (focal type 1 vs. focal type 2)	Infiltrative pRCC[a]	*P* (infiltrative vs. all focal)
Metastatic disease[b]	3.7 (2/54)	7.5 (3/40)	0.648	75.0 (6/8)	**<0.001**
Central location	4.6 (3/65)	5.6 (3/54)	1.0	88.9 (8/9)	**<0.001**
Poorly encapsulated	0 (0/65)	3.7 (2/54)	0.204	100 (9/9)	**<0.001**
Renal vein thrombus	0 (0/65)	0 (0/54)	1.0	88.9 (8/9)	**<0.001**
Irregular margins	21.5 (14/65)	35.2 (19/54)	0.089	100 (9/9)	**<0.001**
Perirenal invasion	6.2 (4/65)	3.7 (2/54)	0.688	55.6 (5/9)	**<0.001**
Retroperitoneal collaterals	30.8 (20/65)	22.2 (12/54)	0.309	77.8 (7/9)	**0.007**
Homogeneous enhancement	46.2 (30/65)	42.6 (23/54)	0.715	11.1 (1/9)	0.084
Microscopic fat[c]	7.9 (5/63)	3.8 (2/53)	0.451	22.2 (2/9)	0.095
Homogeneous T2 signal intensity	35.4 (23/65)	22.2 (12/54)	0.157	11.1 (1/9)	0.264
Haemosiderin[c]	27.0 (17/63)	50.9 (27/53)	0.056	22.2 (2/9)	0.358
Necrosis	32.3 (21/65)	25.9 (14/54)	0.448	55.6 (5/9)	0.117
Haemorrhage	41.5 (27/65)	70.4 (38/54)	**0.004**	22.2 (2/9)	0.082
High grade (most common)	1.5 (1/65)	38.9 (21/54)	**<0.001**	44.4 (4/9)	0.077
High grade (highest)	38.5 (25/65)	88.9 (48/54)	**<0.001**	88.9 (8/9)	0.134
Stage T2/T3	11.1 (7/63)	28.0 (14/50)	**0.022**	87.5 (7/8)	**<0.001**

Data listed in bold are statistically significant at P<0.05. Features not recorded in binary fashion (T2 signal intensity, enhancement in nephron-graphic phase, and cystic component) are not included in the table but did not show significant differences for any comparisons (*P*>0.05)

[a] Data are percentages, with raw numbers in parentheses

[b] Not included in patients for whom presence or absence of metastatic disease could not be determined

[c] Not evaluated in three lesions imaged at 3.0 T with in-phase echo acquired before the opposed-phase echo

Table 3

Accuracy, sensitivity, specificity and odds ratios associated with factors identified as a significant predictor of metastatic disease of papillary renal cell carcinoma (pRCC) at univariate analysis

Feature	Criterion[a]	Odds ratio	Accuracy[b]	Specificity[b]	Sensitivity[b]
Renal vein thrombus	Present	108.0	93.3 (84/90)	98.7 (78/79)	54.5 (6/11)
Location	Central	58.0	92.2 (83/90)	94.9 (75/79)	72.7 (8/11)
MRI appearance	Infiltrative	53.4	92.2 (83/90)	97.5 (77/79)	54.5 (6/11)
Maximum size	>68 mm	45.9	91.1 (82/90)	93.7 (74/79)	72.7 (8/11)
Encapsulation	Poorly encapsulated	35.2	91.1 (82/90)	96.2 (76/79)	54.5 (6/11)
Margins	Irregularity	33.3	76.7 (69/90)	74.7 (59/79)	90.9 (10/11)
T stage	T2/T3	22.1	83.1 (69/83)	83.6 (61/73)	80.0 (8/10)
Perirenal invasion	Present	9.8	86.7 (78/90)	93.7 (74/79)	36.4 (4/11)
Retroperitoneal collaterals	Present	7.9	76.7 (69/90)	77.2 (61/79)	72.7 (8/11)
Pathological type	Type 2	6.0	57.8 (52/90)	54.4 (43/79)	81.8 (9/11)
Most common nuclear grade	High	4.6	78.9 (71/90)	83.5 (66/79)	45.5 (5/11)

[a] For patients with multiple pRCC, the patient was considered to test positive for the criterion if the criterion was satisfied in at least one lesion

[b] Data are percentages, with raw numbers in parentheses